Determination of BO-LID and LeTID Related Activation Energies in Cz-Si and FZ-Si using Constant Injection Conditions

Alexander Graf[a)], Axel Herguth[b)] and Giso Hahn[c)]

University of Konstanz, Department of Physics, 78457 Konstanz, Germany

[a)]Corresponding author: alexander.graf@uni-konstanz.de
[b)]axel.herguth@uni-konstanz.de
[c)]giso.hahn@uni-konstanz.de

Abstract. Activation energies for the regeneration of BO-LID differ strongly in literature. Two possible reasons, among others, are suspected to cause this spread in published data. On the one hand, ignoring the injection dependence of the reactions might lead to varying results. On the other hand, the parallel occurrence of LeTID might play a role. While the first reason is eliminated within this contribution by keeping injection constant during the degradation and regeneration treatment, LeTID is indeed found to occur and impact the degradation and regeneration in Cz-Si as can be seen from extracted defect densities and injection-dependent lifetime data. In FZ-Si which is supposed to suffer from LeTID only, activation energy for degradation and regeneration was determined to be $E_{a,deg} = 0.78 \pm 0.09$ eV and $E_{a,reg} = 0.62 \pm 0.09$ eV independent of firing temperature. For Cz-Si, activation energy of degradation is found to depend slightly on firing temperature, probably due to the superposition of BO-LID with LeTID. Activation energy of regeneration of both, FZ-Si and Cz-Si, is found to be the same within uncertainty. The results furthermore suggest that the superposition of BO-LID and LeTID is not responsible for the broad range of published activation energies.

INTRODUCTION

Studies on boron-oxygen related light-induced degradation (BO-LID) usually do not take care of light- and elevated temperature-induced degradation (LeTID) which was first described in multicrystalline (mc) Si [1] and later also found in Czochralski (Cz) Si [2] and Floatzone (FZ) Si [3]. The occurrence of BO-LID and LeTID in parallel could be an explanation for various different activation energies found in the context of BO-LID and its regeneration [4, 5]. Another problem is that the various defect reactions depend on injection [6] which is not constant during treatment due to changing lifetime when constant illumination is used [7]. In this study the occurrence of LeTID in Cz-Si and how it affects experiments on BO-LID is investigated. Activation energies depending on firing temperature for FZ-Si and Cz-Si are determined under constant injection rather than constant illumination conditions. As LeTID is becoming stronger with increasing firing temperatures [8], different firing settings have been investigated.

EXPERIMENTAL DETAILS

Lifetime samples were prepared using FZ- and Cz-grown boron-doped wafers with a doping level p_0 of $(9.8 \pm 0.7) \times 10^{15}$ cm^{-3} (corresponding to a resistivity of 1.5 ± 0.1 Ωcm) for Cz-Si and $7.2 \pm 0.4 \times 10^{15}$ cm^{-3} (2.0 ± 0.1 Ωcm) for FZ-Si. Wafers were first etched to remove saw damage in an aqueous solution of KOH (22 %, ~80 °C) followed by a short chemical polish at room temperature in a solution of HNO_3 (65 %), acetic acid (99.8 %) and HF (50 %) in a ratio of 29:5:3. Thereafter, an oxide was grown wet-chemically in a solution of H_2O_2 (30 %) and H_2SO_4 (96 %) in a ratio of 1:3 at ~80 °C, which was afterwards stripped in diluted HF (2 %) to remove surface contaminations (Piranha clean). A phosphorus-doped emitter is created via $POCl_3$ diffusion (~80 Ω/□) and etched back to ~100 Ω/□ in a solution of HF (50 %), HNO_3 (65 %) and H_2O (ratio 1:9:38) in order to reduce the emitter related

Konstanzer Online-Publikations-System (KOPS)
URL: http://nbn-resolving.de/urn:nbn:de:bsz:352-2-v28178p6o6xu4

SiliconPV 2019, the 9th International Conference on Crystalline Silicon Photovoltaics
AIP Conf. Proc. 2147, 140003-1–140003-5; https://doi.org/10.1063/1.5123890
Published by AIP Publishing. 978-0-7354-1892-9/$30.00

recombination losses. The resulting porous silicon is removed in an aqueous solution of KOH (0.5 %, room temperature). After processing the final thickness of the wafers is 145 ± 5 µm (Cz-Si) and 152 ± 5 µm (FZ-Si). The samples were passivated by a hydrogen-rich amorphous silicon nitride (SiN_x:H) on both sides using a direct plasma-enhanced chemical vapor deposition (PECVD) at a temperature of 450 °C. Samples are then fired at measured peak temperatures between 750 °C and 900 °C in a fast firing furnace. Prior to and during degradation treatment, effective excess carrier lifetime τ_{eff} was measured at 30 °C with a WTC-120 lifetime tester and at treatment temperature (>30 °C) using a WCT-120TS lifetime tester from Sinton Instruments [9]. All samples were degraded and regenerated at temperatures between 80 °C and 150 °C using a widened, homogenized laser beam at 800 − 805 nm at varying intensity in order to reach constant injection as described below. Sample temperature is measured by a thermal camera (A655SC, FLIR) and held stable during illumination using a hotplate. During the treatment the samples were temporarily removed between illumination steps to determine τ_{eff}. Each measurement series was continued until $\tau_{\text{eff}}(t)$ almost reached its initial value again.

Method for Treatment at Constant Injection

Using constant illumination conditions, *i.e.*, constant generation rate G, during degradation treatments, the minority carrier density $\Delta n = \tau_{\text{eff}} \cdot G$ varies due to degradation of effective lifetime τ_{eff}. For the sample shown in Fig. 1 (left) τ_{eff} varies from ∼36 µs to ∼180 µs, thus Δn varies from $\sim 5 \times 10^{14}\,\text{cm}^{-3}$ to $\sim 3 \times 10^{15}\,\text{cm}^{-3}$ at a photon flux equivalent to 1 sun [10]. This strong variation prevents accurate fitting of degradation and regeneration via two exponential functions (blue data and line in Fig. 1 right) shown to describe defect dynamics assuming constant transition rates [11]. Adjusting light intensity or rather $G = \Delta n / \tau_{\text{eff}}$ in order to keep Δn constant leads to a superior fit result (red data and line in Fig. 1 right).

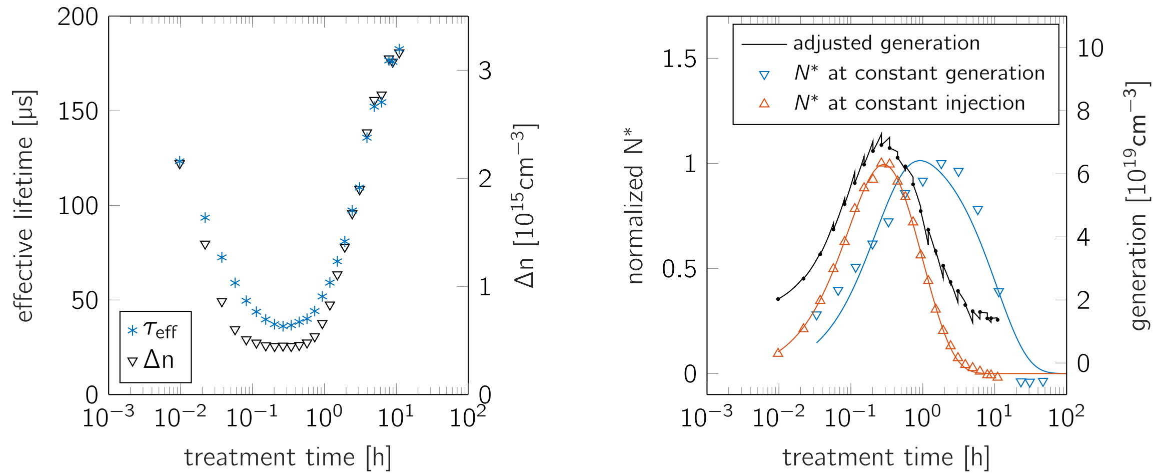

FIGURE 1. Left: τ_{eff} at $\Delta n = 1 \times 10^{15}\,\text{cm}^{-3}$ and calculated Δn during treatment for constant illumination at 1 sun. Note that Δn is not directly proportional to τ_{eff} due to the dependency of τ_{eff} on Δn. Right: Comparison of defect density between constant illumination (1 sun) and constant injection ($2.5 \times 10^{15}\,\text{cm}^{-3}$).

It is important to note that $\tau_{\text{eff}}(T)$ depends on temperature (T) and thus adjustment of G during degradation requires τ_{eff} to be determined at treatment temperature. Changes in τ_{eff} during degradation are monitored by intermittent ex-situ photoconductance decay measurements, after which intensity is adapted. A linear extrapolation from the previous points is used to adjust intensity between measurements (black data in Fig. 1 right).

RESULTS

SRH Defect Analysis and Defect Density

Assuming that during degradation and regeneration only one defect species in the bulk forms and vanishes, an injection-dependent correlated lifetime τ_{def} can be isolated

$$N^* = \frac{1}{\tau_{def}(t)} = \frac{1}{\tau_{eff}(t)} - \frac{1}{\tau_{eff}(0)} \tag{1}$$

also defining an equivalent defect density N^* (in s^{-1}) being proportional to the actual defect density N (in cm^{-3}). Surface passivation layers on an emitter have been shown to be fairly stable which allows this approach [12]. The maximum defect density reached during degradation is shown in Fig. 2 (left). For both, FZ-Si and Cz-Si, defect density increases with firing temperature.

In order to find out which defect predominantly forms with increasing firing temperature, injection-dependent lifetime data $\tau_{def}(\Delta n)$, described using Shockley-Read-Hall (SRH) theory [13, 14], is evaluated. Since BO-LID and LeTID may affect the lifetime simultaneously, $\tau_{def}(\Delta n)$ includes both defects and two SRH functions would be needed for accurate description. However, this leads to a multitude of free fitting parameters probably without physical meaningful information. Thus only one hypothetical defect is fitted with the assumption that the defect is deep (defect level in the center of the band gap) and known doping. Then only the apparent hole and electron capture times τ_p and τ_n are free parameters for fitting and a quite stable fit is possible. The obtained ratio $k = \tau_p/\tau_n$ is an effective ratio k_{eff} for the combination of multiple defects. If one defect dominates, k_{eff} is near k of this defect. For a mixture of both, k_{eff} is in between the k values of the individual defects. Fig. 2 (right) shows the ratio obtained for different firing temperatures.

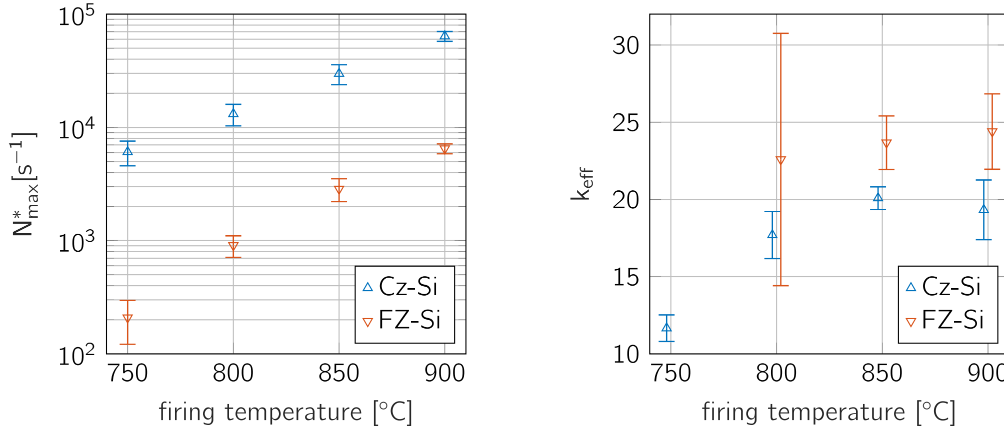

FIGURE 2. Left: Maximum defect density N^* at $\Delta n = p_0/10$ in dependence of firing temperature. Right: Determined k_{eff} at maximum defect density for FZ-Si and Cz-Si samples depending on firing temperature.

For high firing temperatures k_{eff} of Cz-Si approaches k_{eff} of FZ-Si which indicates that the same defect starts to form with increasing temperature and dominates over the BO defects ($k \approx 10$) which leads to an increasing k_{eff}. Thus increasing defect density in Fig. 2 (left) can be attributed to LeTID in both, Cz-Si and FZ-Si. At 750 °C no k_{eff} could be determined for FZ because degradation is too weak.

Instead of only determining k_{eff} at maximum defect density, it is possible to determine it throughout the treatment in order to get a time-resolved k_{eff}. Since degradation and regeneration rate can differ between LeTID and BO-LID, k_{eff} is expected to change over time due to a varying ratio of BO and LeTID related defect densities. As shown in Fig. 3, k_{eff} of the sample fired at T_{fire} = 800 °C significantly changes over time from around 10 to over 20 indicating that at the beginning BO-LID is the dominant defect and over time LeTID becomes the limiting defect, thus showing that LeTID kinetics are slower compared to BO-LID at 80 °C treatment temperature. For the sample fired at T_{fire} = 750 °C the same happens, however, k_{eff} stays closer to 10 throughout most of the treatment. Due to increased severity of LeTID with increasing firing temperature, k_{eff} changes only slightly at T_{fire} = 850 °C and stays around 20 throughout the whole treatment.

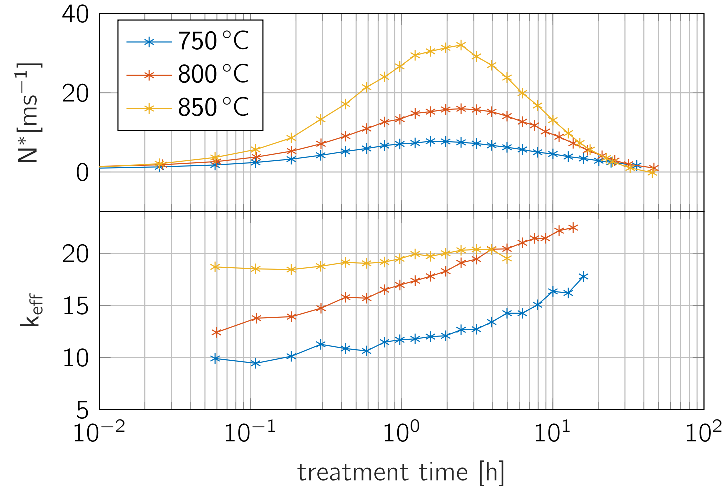

FIGURE 3. Time evolution of k_{eff} and N^* at $\Delta n = p_0/10$ of Cz-Si samples treated at 80 °C.

Activation Energy of Degradation and Regeneration

In order to determine activation energies for the FZ-Si and Cz-Si samples fired at 700, 800 and 850 °C, degradation and regeneration rates during the degradation treatment at various temperatures ranging from 80 °C to 150 °C are extracted from N^* using a double exponential fit (see Fig. 1 right). Via an Arrhenius plot apparent activation energies E_{a} of degradation and regeneration are determined from these rates (example in Fig. 4 left).

For degradation (Fig. 4 middle) in Cz-Si fired at $T_{\mathrm{fire}} = 750$ °C the observed value $E_{\mathrm{a}} = 0.547 \pm 0.024$ eV does not match the one of BO-LID in literature $E_{\mathrm{a}} = 0.475 \pm 0.035$ eV [15]. This can be explained by a small influence of LeTID which already occurs at $T_{\mathrm{fire}} = 750$ °C as shown in the time evolution of k_{eff}. At higher firing temperatures E_{a} of Cz-Si approaches E_{a} of FZ-Si with a value of approx. $E_{\mathrm{a,Cz}} = 0.73$ eV. Due to a non-negligible influence of BO-LID, E_{a} of Cz-Si always stays below E_{a} of FZ-Si. Activation energy of regeneration does not differ significantly between firing temperatures or between FZ-Si and Cz-Si. Thus it looks as if E_{a} of regeneration for both, BO-LID and LeTID, are close to each other maybe suggesting a common mechanism of action.

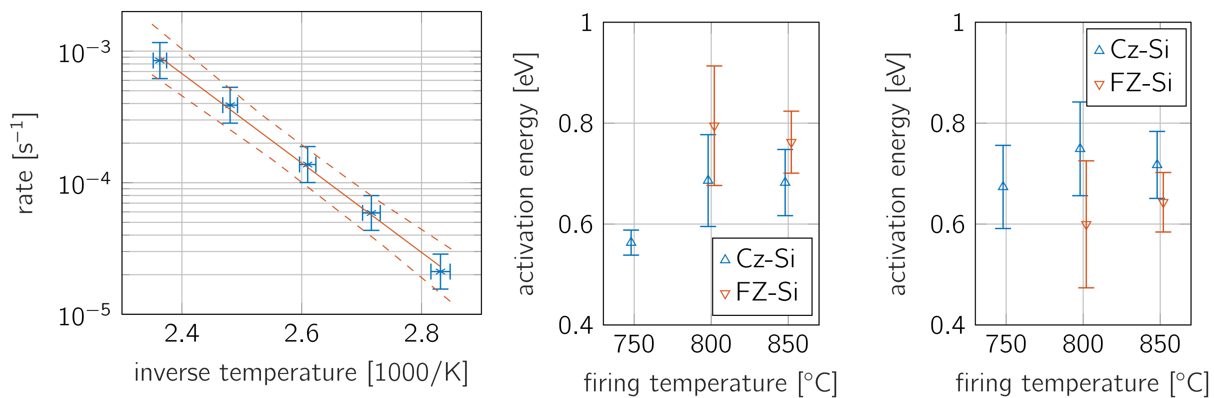

FIGURE 4. left: Example for Arrhenius plot for regeneration of Cz-Si fired at 750 °C. The dashed lines show the interval where 95 % of the values are expected to be in between. The central fit results in $E_{\mathrm{a}} = 0.68 \pm 0.08$ eV. middle: Activation energy of degradation. right: Activation energy of regeneration.

CONCLUSIONS

Depending on firing temperature, LeTID occurs with varying strength in Cz-Si and FZ-Si. Via k_{eff} it is possible to identify the dominating defect in Cz-Si, LeTID or BO-LID. Using constant injection conditions for degradation and regeneration, more accurate fitting of defect density is possible eliminating a possible error source for determination of activation energies. For degradation, activation energy of LeTID and BO-LID differs. For regeneration no difference has been observed, thus, the wide range of activation energies for BO regeneration cannot be explained by an influence of LeTID during experiments on BO-LID.

ACKNOWLEDGMENTS

Part of this work was supported by the German Federal Ministry for Economic Affairs and Energy under contract numbers 0324080C and 0324001. The content is the responsibility of the authors.

REFERENCES

[1] K. Ramspeck, S. Zimmermann, H. Nagel, A. Metz, Y. Gassenbauer, B. Birkmann, and A. Seidl, "Light induced degradation of rear passivated mc-si solar cells," in *Proc. 27th EUPVSC* (2012), pp. 861–865.

[2] F. Fertig, R. Lantzsch, A. Mohr, M. Schaper, M. Bartzsch, D. Wissen, F. Kersten, A. Mette, S. Peters, A. Eidner, J. Cieslak, K. Duncker, M. Junghänel, E. Jarzembowski, M. Kauert, B. Faulwetter-Quandt, D. Meißner, B. Reiche, S. Geißler, S. Hörnlein, C. Klenke, L. Niebergall, A. Schönmann, A. Weihrauch, F. Stenzel, A. Hofmann, T. Rudolph, A. Schwabedissen, M. Gundermann, M. Fischer, J. Müller, and D. Jeong, Energy Procedia **124**, 338–345 (2017).

[3] T. Niewelt, F. Schindler, W. Kwapil, R. Eberle, J. Schön, and M. C. Schubert, Prog. Photovolt. Res. Appl. **26**, 533–542 (2017).

[4] A. Herguth, G. Schubert, M. Kaes, and G. Hahn, "A new approach to prevent the negative impact of the metastable defect in boron doped CZ silicon solar cells," in *Proc. WCPEC-4* (2006), pp. 940–943.

[5] B. Lim, K. Bothe, and J. Schmidt, Semicond. Sci. Technol. **26**, p. 095009 (2011).

[6] A. Herguth, G. Schubert, M. Kaes, and G. Hahn, Prog. Photovolt. Res. Appl. **16**, 135–140 (2008).

[7] D. C. Walter, L. Helmich, D. Bredemeier, R. Falster, V. V. Voronkov, and J. Schmidt, "Lifetime evolution during regeneration in boron-doped czochralski-silicon," in *Proc. 35th EUPVSC* (2018), pp. 522–526.

[8] D. Chen, M. Kim, B. V. Stefani, B. J. Hallam, M. D. Abbott, C. E. Chan, R. Chen, D. N. Payne, N. Nampalli, A. Ciesla, T. H. Fung, K. Kim, and S. R. Wenham, Sol. Energy Mat. Sol. Cells **172**, 293–300 (2017).

[9] R. Sinton, A. Cuevas, and M. Stuckings, "Quasi-steady-state photoconductance, a new method for solar cell material and device characterization," in *Proc. 25th IEEE PVSC* (1996), pp. 457–460.

[10] A. Herguth, Energy Procedia **124**, 53–59 (2017).

[11] A. Herguth and G. Hahn, J. Appl. Phys **108**, p. 114509 (2010).

[12] D. Sperber, A. Schwarz, A. Herguth, and G. Hahn, Sol. Energy Mat. Sol. Cells **188**, 112–118 (2018).

[13] W. Shockley and W. T. Read, Phys. Rev. **87**, 835–842 (1952).

[14] R. N. Hall, Phys. Rev. **87**, 387–387 (1952).

[15] K. Bothe and J. Schmidt, J. Appl. Phys **99**, p. 013701 (2006).